Numerical Simulation of Superconformal Electrodeposition Using the Level Set Method

D. Wheeler, D. Josell and T.P. Moffat (NIST)

National Institute of Standards and Technology,
100 Bureau Drive, Stop 8555,
Gaithersburg, MD 20899-8555,
e-mail: Daniel.Wheeler@nist.gov

ABSTRACT

Damascene copper is rapidly replacing aluminum as the interconnect material of choice in silicon technology. The change is driven by the lower electrical resistivity of copper, which decreases power consumption and permits increased central processor unit (CPU) clocking speeds. Electroplating is the preferred deposition method because it permits filling of high-aspect ratio features without seams or voids through the process of superconformal deposition, also called "superfill." This process only occurs when particular combinations of chemical additives are included in the electrolyte [1]. Two crucial mechanisms by which the additives enable superfill to occur are (a) accelerator behavior increasing the copper deposition rate as a function of coverage and (b) conservation of accelerator coverage with increasing/decreasing arc length [2]. The model presented here utilizes the level set method (LSM) to track the position of the copper/electrolyte interface as the features are filling.

Keywords: level set method, electrodeposition, numerical method, electrolyte, scalar variable, interface tracking

1 INTRODUCTION

"Curvature enhanced accelerator coverage" (CEAC) has been proposed as the mechanism behind superconformal filling. This mechanism depends critically on the additive composition and concentration in the electrolyte. Both an inhibitor and accelerator species must be present with the latter comparatively dilute. The additives must behave as adsorbates forming a monolayer at the metal/electrolyte interface. The high concentration of inhibitor means initial negligible accelerator content in the monolayer resulting in a short period of conformal deposition. The accelerator must have the inherent ability to displace the inhibitor allowing slow coverage build up on the interface. When the accelerator content in the monolayer becomes significant, arc length evolution along the interface results in changing surface coverage of the accelerator. Areas of high positive curvature (concave) increase local coverage while high negative curvature decreases coverage. This enables a differential deposition rate between the bottom surface and side walls of the trench. The rate of accelerator build up is crucial with over concentrated or dilute accelerator preventing superfill. Further details of additive constituents and experimental determination of concentrations can be found in refs [1], [3].

Previous modeling of copper deposition utilized leveling theory that only considered spatially varying accumulation of inhibiting additives induced by concentration gradients within the electrolyte [4]–[6]. However, such leveling theories could not self-consistently explain superconformal filling of sub-micron, high-aspect ratio features. With all leveling models, rapid deposition also occurs on the sides approaching the bottoms of the features, rather than only on the bottom as is generally acknowledged to be the case in experimental studies. Furthermore, leveling models do not predict an incubation period of conformal growth prior to superfill or development of a bump over the features after superfill, both well known experimentally.

This paper presents a computational solution to the superfill modeling problem. The Level Set Method (LSM) is used to track the copper/electrolyte interface on a rectangular grid. Determination of the time-dependent accelerator coverage adsorbed on the interface is accomplished by evolution of a scalar concentration variable defined throughout the domain. Comparison is shown between experimental fill and simulation results.

2 MODEL SPECIFICATION

The local interface velocity is expressed in terms of the local deposition current density i by [2],

$$\vec{v} = \frac{i \Omega \vec{n}}{2F}, \tag{1}$$

where $\vec{n}$, Ω and F are the normal to the interface pointing into the electrolyte, the atomic volume and Faraday's constant respectively. The 2 is the cupric ion charge (Cu^{2+}). The current density i is given by the Butler-Volmer equation [2],

$$i = i_0 \frac{c_c^i}{c_c^\infty} \exp(-\frac{\alpha F}{RT} \eta), \tag{2}$$

where i_0, c_c^i, c_c^∞, α, R, T and η are the exchange current density, the molar concentration of copper at the

interface, the molar concentration of copper in the far field, the transfer coefficient (a measure of the symmetry of the energy barrier), the gas constant, the temperature and the overpotential respectively. Dependence of Eq. (2) on the accelerator coverage adsorbed at the metal/electrolyte interface, θ, is determined experimentally from (i-η) studies of deposition on flat copper electrodes independent from trench filling experiments. The dependencies are given by [2], [3],

$$i_0(\theta) = b_0 + b_1\theta, \tag{3}$$

and

$$\alpha(\theta) = m_0 + m_1\theta. \tag{4}$$

The rate of change of accelerator coverage, θ, depends on the interface arc length evolution and the adsorption from the electrolyte. This evolution is expressed by,

$$\dot{\theta} = Jv\theta + \frac{k}{\Gamma_0}(1-\theta)c_m^i, \tag{5}$$

where J, k, c_m^i, Γ_0 are the curvature, the jump potential, the accelerator molar concentration in the electrolyte at the interface and the site density on the interface respectively. Also $\vec{v} = v\vec{n}$ with $v = |\vec{v}|$. The jump potential varies with the overpotential η such that

$$k(\eta) = k_0 - k_3\eta^3. \tag{6}$$

The parameter values for Eqs. (3), (4) and (6), obtained entirely from (i-η) voltammetry on flat copper electrodes [2], are listed in Table 1. The concentration

Parameter	*Value*	*Unit*
b_0	0.069	A/m^2
b_1	6.4	A/m^2
m_0	0.447	dimensionless
m_1	0.299	dimensionless
k_0	0.18	m/s^{-1}
k_3	25.0	m/sV^3
Γ_0	9.7×10^{-6}	mol/m^2

Table 1: Experimental parameters obtained by best fit analysis of cyclic voltammetry to determine θ dependence. The site density γ_0 is for site packing on a copper surface.

of the cupric and accelerator in the electrolyte are governed by diffusion such that,

$$\frac{\partial c_\xi}{\partial t} = D_\xi \nabla^2 c_\xi, \tag{7}$$

where t is time and $c_\xi = c_\xi^\infty$ outside of the boundary layer of depth δ. The subscript ξ is given by

$$\xi = \begin{cases} m, & \text{for accelerator,} \\ c, & \text{for Cu}^{2+}. \end{cases} \tag{8}$$

The flux loss from the electrolyte at the interface is given by

$$-D_\xi \frac{\partial c_\xi}{\partial n} = \begin{cases} -k(1-\theta)c_m^i, & \text{for accelerator,} \\ -v(V_c - c_c^i), & \text{for Cu}^{2+}, \end{cases} \tag{9}$$

where V_c is the molar volume of solid copper. The aspect ratio of the trench and the trench spacing are given by $B/2A$ and $2w$ respectively. The main approximation of the model geometry compared with the experimental configuration is the assumption of an infinite set of trenches. Typically experimental configurations consisted of ≈100 trenches with $w \approx 1$ μm. The model symmetry condition is a good approximation under these conditions.

The finite difference equations are derived for a non-uniform cell-centered rectangular mesh using the Finite Volume method as first introduced by Patankar [7]. A control volume formulation is used, at whose center the variables are being evaluated [8].

In the level set the variable, $\phi = 0$ marks the position of the interface. It is continuous and monotonic in the region near the interface. An advection equation is then used to describe the motion of the interface. Further details of the discretisation, the level set method and validation of the model used in this paper can be found in ref [10].

3 Modeling and Experimental Comparison

Interface evolution for a variety of deposition and geometric parameters was simulated for comparison with experimental results. The goal was to predict a parameter space, (η, c_m^∞), for which superfill occurs at high aspect ratios. The type of filling, ranging from conformal to superfill, can be determined from the presence/absence of voids in the filled trench as well as features, such as cusps and bumps, that form above the trench during deposition. Experimentally, there is some variation in the formation of these features under nominally identical conditions due to uncontrolled experimental differences. However it is generally clear when superfill occurs for particular parameters. For example, the superfill behavior in Figure 1(c) manifests as both trench filling and an overfill bump that are experimentally reproducible. Both filling and deposition features can be used for semi-quantitative determination of model accuracy.

In the experiments, Figure 1, the aspect ratios of the patterned trenches are approximately 1.5, 1.9, 2.5, 3.3 and 4.6 with a trench depth of 0.46 μm. The first set of trenches, Figure 1(a), show the poor filling that occurs when no additive is present in the electrolyte, $c_m^\infty = 0$. Voids are evident in all trenches. The filling is conformal until the unfilled region of the trench

becomes sufficiently narrow that the deposition rate decreases going down the trench. The differential deposition rate causes the sidewalls to bulge and neck near the top of the trench creating a void. Voiding in the second set of trenches, Figure 1(b), is significantly reduced by the inclusion of additives in the electrolyte. Selection of near optimal additive concentrations leads to optimal filling, Figure 1(c). Excessive additive concentration results in a reversion to conformal deposition, Figure 1(d). Trenches which contain voids characteristically have a cusp over them while those that fill have a bump. Trenches without a void but with a cusp above them, (Figure 1(d) aspect ratio 2), typically contain a seam or a very thin void. Parameters that correspond

Parameter	*Value*	*Unit*
B	0.46	μm
w	5.0	μm
c_c^∞	250.0	mol/m^3
V_c	0.141×10^6	mol/m^3
Γ_0	9.8×10^6	mol/m^2
σ_{cfl}	0.1	
δ	1.5×10^{-5}	m
D_{cu}	5.0 ×10^{-10}	m^2/s
D_{mpsa}	1.0 ×10^{-9}	m^2/s

Table 2: Material and geometric parameters used for the simulations for comparison with experiment.

to the experimental conditions are presented in Table 2. Simulations were performed using the values contained in Tables 1 and 2 with the exception of the trench depth B which was modeled as 0.5 μm. Also the trench spacing was modeled with a value of $w = 5$ μm, giving only slight overlap of diffusion fields, due to the small fraction of the specimen surface area that was perturbed due to trench patterning. The simulations, Figure 2 show good agreement with experiment, accurately predicting the formation of voids, cusps and bumps. For the ($\eta = -0.301$, $c_m^\infty = 0.0005$) case, see Figure 2, deposition is predicted to be conformal. The large overpotential leads to a high base velocity ($v(\theta)$ at $\theta = 0$), Eq. (2), and thus, due to dilute accelerator concentration, close-off occurs before the CEAC mechanism becomes significant. This leads to voids particularly in all the trenches. In the ($\eta = -0.15$, $c_m^\infty = 0.04$) case, Figure 2, significant acceleration by the CEAC mechanism occurs at the bottom of the trench as required for superfill. However, accelerator coverage on the sidewalls builds up almost as quickly through simple accumulation due to the high accelerator concentration in the electrolyte. This effect is aggravated by the slow base velocity at low overpotentials. This leads to a seam in the trench of aspect ratio 2 and voids in the other trenches. In the ($\eta = -0.282$, $c_m^\infty = 0.005$) case, superfill is predicted to occur for all but the finest feature. Here the accumulation and overpotential dependent base velocity combined appropriately to give rapid enhancement of accelerator coverage only on the bottom of the filling feature. Though the experimental image, Figure 1(c), appears to indicate fill in all features for these conditions, it is likely that the finest feature does in fact contain a fine seam [1].

The simulations were performed with mesh densities of 300 by 55, 300 by 45, 300 by 39, 300 by 30 and 300 by 24 elements for the 2, 2.5, 3, 4 and 5.6 aspect ratio features, respectively. These simulations took between 1 and 5 hours on a 500 MHz processer.

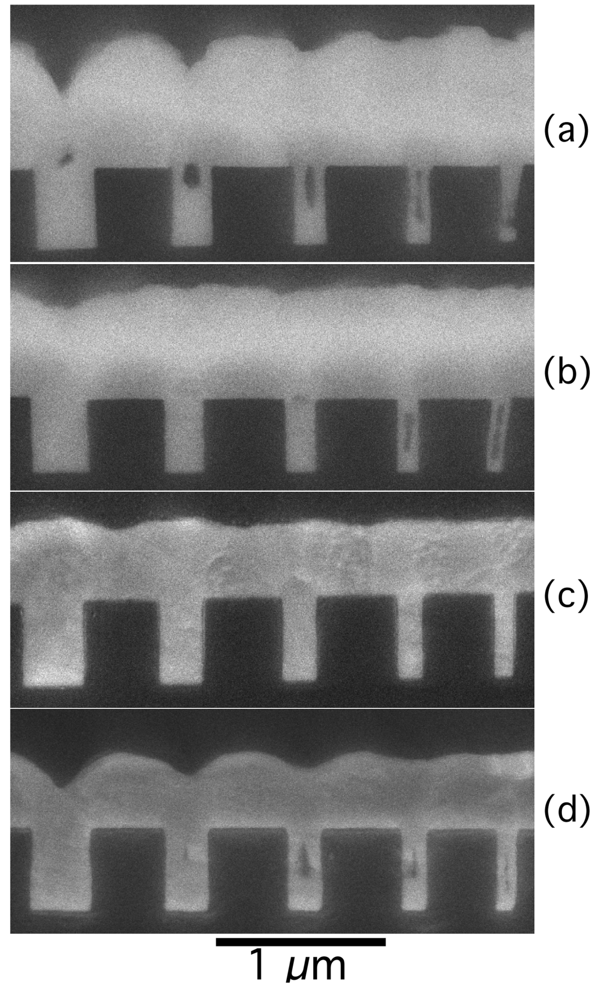

Figure 1: Scanning electron microscope images of trenches filled from electrolytes with c_m^∞: 0, 0.0005, 0.005 and 0.04 mol/m^3 and overpotentials η: -0.097, -0.301, -0.282 and -0.150 V (top to bottom), and aspect ratios (with Cu seed): 2.0, 2.5, 3.0, 4.0, 5.6 (left to right).

REFERENCES

[1] T.P. Moffat and J.E. Bonevich and W.H. Huber and A. Stanishevsky and D.R. Kelly and G.R. Stafford and D. Josell, “Superconformal Electrodeposition of Copper in 500-90 nm Features”, J. Electrochem. Soc., 147, 12, 4524-4535, 2000.

[2] D. Josell and D. Wheeler and W.H. Huber and T.P. Moffat, “Superconformal Electrodeposition in Submicron Features”, Phys. Rev. Lett., 87, 1, 016102-1–016102-4, 2001.

[3] T.P. Moffat and D. Wheeler and W.H. Huber and D. Josell, “Superconformal Electrodeposition of Copper”, Electrochem. Solid-State Lett., 4, 4, C26-C29, 2001.

[4] P.C. Andricacos and C. Uzoh and J.O. Dukovic and J. Horkans and H. Deligianni, ”Damascene Copper Electroplating for Chip Interconnections”, IBM J. of Research Development, 42, 5, 567-573, 2001.

[5] A.C. West, ”Theory of Filling of High-Aspect Ratio Trenches and Vias in Presence of Additives”, J. Electrochem. Soc., 147, 1, 227-232, 2000.

[6] C. Madore and M. Matlosz and D. Landolt, ”Blocking Inhibitors in Cathodic Leveling”, J. Electrochem. Soc., 143, 7, 1996.

[7] S.V. Patankar and D.B. Spalding, ”A Calculation Procedure for Heat, Mass and Momentum Transfer in Three-Dimensional Parabolic Flows”, International J. of Heat and Mass Transfer, 15, 1787-1806, 1972.

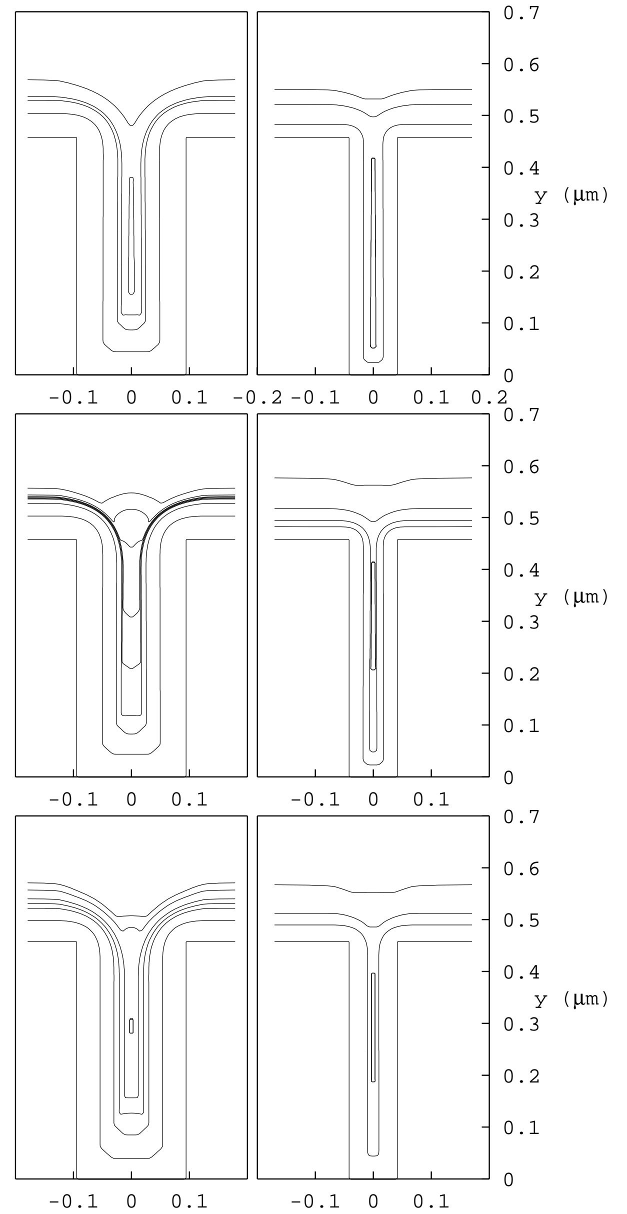

Figure 2: Simulations of copper deposition in trenches with aspect ratios (left to right) of 2.0, 2.5, 3.0, 4.0 and 5.6. The overpotential and and accelerator concentration (top to bottom) are $\eta = -0.301$ V and $c_m^\infty = 0.0005$ mol/m^3, $\eta = -0.282$ V and $c_m^\infty = 0.005$ mol/m^3 and $\eta = -0.15$ V and $c_m^\infty = 0.04$ mol/m^3 respectively.